FEATURE ARTICLE

Geothermal Vents and Chemical Processing: The Infrared Spectroscopy of Hydrothermal Reactions

Thomas B. Brill

Department of Chemistry and Biochemistry, University of Delaware, Newark, Delaware 19716

Received: October 21, 1999; In Final Form: January 6, 2000

Water at high pressure and high temperature (hydrothermal conditions) is prevalent in geochemistry and may have contributed to the origin of life. On the practical side, hydrothermal methods are useful in selected applications for organic and inorganic synthesis, biomass conversion, and aqueous waste stream remediation. An overview is presented of fundamental research from this laboratory that is intended to underpin these fields. The objective is to determine the kinetics and outline the pathways of broadly applicable aqueous organic and inorganic reactions at the conditions of 373−623 K and 275 bar. The main approach employs IR spectroscopy in conjunction with a thin-film flow reactor for real-time, in situ observations of the species. Supplemental studies with Raman spectroscopy help identify the components. The molecular focus is on reactants that possess functional groups with universal implications for organic chemistry in water, e.g., amines, carboxylates, and nitriles.

Introduction

Fluid water at high pressure and temperature is closely allied with many natural and industrial processes. The term "hydrothermal" frequently is used to describe water at these conditions. The more specific label of "supercritical" refers to the state in which the critical temperature (647 K) and the critical pressure (221 bar) are simultaneously exceeded. Hydrothermal conditions are widespread in the crust of the earth. Eye-catching geothermal vents first witnessed in the late 1970s[1−4] occur in sub-sea rift zones where depths of 2000 m or more produce hydrostatic pressures that exceed the critical pressure of pure H_2O. These pressures along with particulate minerals and temperatures of 573−625 K have given rise to the popular name "black smokers". A fascinating feature of sea floor vents is the observation that universally prevalent source molecules (e.g., CO, CO_2, CH_4, NH_3, H_2O, H_2S, H_2, etc.) react to synthesize larger molecules (e.g., carboxylic acids,[5−7] amino acids,[8] aldehydes,[9] metal carboxylates,[10] etc.). Because these products are richer in energy, they become food for various organisms and thereby contribute to the existence of a complex ecosystem in the vicinity of many geothermal vents.[11] Based in part on these observations, reactions at hydrothermal conditions may have contributed to the origin of life on this planet and possibly elsewhere.[12−14]

Hydrothermal conditions increasingly find use in industrial processes. Of course, steam has been used for a long time to produce work and to clean materials, but hydrothermally based methods are gaining acceptance for molecular manipulations, such as in aqueous waste stream remediation,[15,16] chemical synthesis,[17] and biomass conversion.[18−21] These technologies make use of the fact that it is easy to tune the solvent and reaction properties of water simply by changing the temperature and pressure in a closed vessel. For example, the bulk dielectric constant decreases from 80 at room temperature to a dimethyl ether-like value of about 6 at the critical point.[22] The ion product of water (pK_w) increases from 14 at room conditions to a peak value of about 10−11 as the critical point is approached,[23] which facilitates acid−base catalyzed reactions. K_w then decreases rapidly in the supercritical region.

Most of the knowledge about reactions at hydrothermal conditions has been obtained from off-line chemical analysis following conversion in a batch or flow reactor. Dynamic, real-time analysis, however, has greater appeal in physical chemistry and can be expected to deepen insight into the details of hydrothermal reactions. Unfortunately, such direct measurements when made spectroscopically require considerable effort, especially when the rates of reactions are sought. Many practical problems arise including the fact that hydrothermal water reacts with most materials commonly used to construct spectroscopy cells. This deleterious property is enhanced by the presence of certain inorganic ions. Hence the durability of the cell components, robustness of the seals, and the possibility of vapor−fluid−solid phase separations are among the potential sources of trouble. In addition, gaps in fundamental knowledge exist, such as the fact that the spectral characteristics of most solute molecules in aqueous solution are not known at high temperature. As these problems are gradually overcome, a variety of readily available spectral methods (e.g., IR[24−36] Raman,[37−41] electronic[42,43]) are being used to characterize reactions at hydrothermal conditions. Each of these spectral methods has strengths and weaknesses, and the process of interest best dictates the choice. For example, the usefulness of the spontaneous Raman effect to study aqueous solutions has long been recognized, and mainly arises from the small differential scattering cross section of H_2O in the bulk compared to most solute molecules. Highly accurate absolute concentration mea-

10.1021/jp993757p CCC: $19.00
Published on Web 03/24/2000

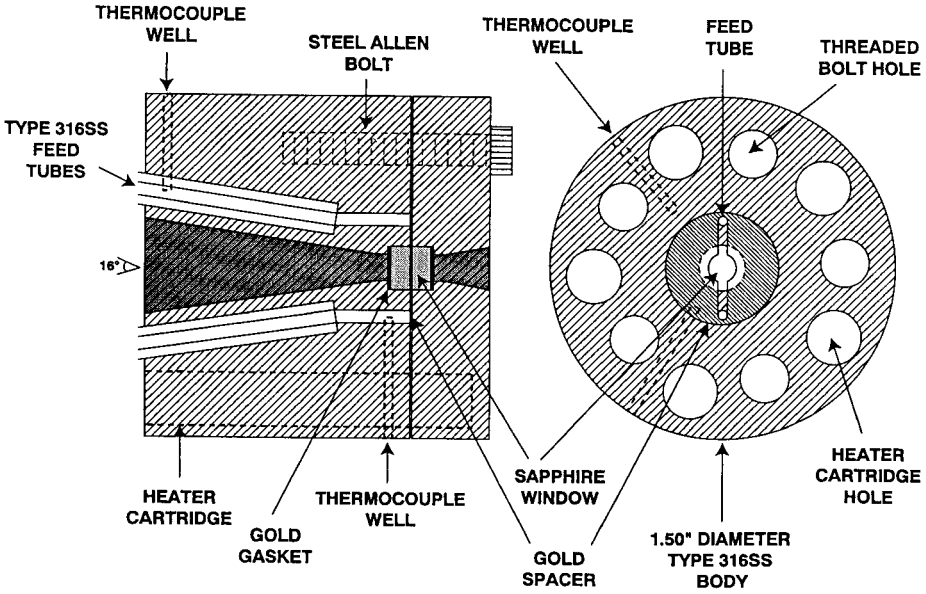

Figure 1. Side and cross sectional views of the 316-SS flow reactor-IR cell containing sapphire windows. Pt−Ir and Ti cells have similar designs. A thin sheet of fluid is created through which the IR beam passes.

surements however can be difficult to obtain from Raman spectra at hydrothermal conditions. By comparison, IR spectroscopy of aqueous solutions is hampered by the large absorptivity of bulk H_2O, but usually benefits from a higher S/N and a simpler physical effect compared to Raman scattering. Hence, quantitative conversion of the band area directly into the absolute concentration is frequently more certain.

Transmission IR spectra can be obtained through a thin sheet of fluid that is created in an optically accessed flow reactor. In this way species are quantifiable in real-time during hydrothermal reactions. Although numerous reactions could be studied, the philosophy behind those chosen is their potential for generality in natural and human-created hydrothermal environments. More specifically, the prevalence of the above-mentioned, relatively stable small molecules in lithospheric and industrial hydrothermal processes suggests that reactions leading to and from these species are universally applicable. The carboxylate and amine functional groups arguably are the most relevant for organic chemistry in water. Development of hydrothermal reaction networks and kinetics leading to and from these functional groups in lower molecular weight molecules is the objective of the work overviewed here.

Experimental Considerations

As alluded to above, many complications confront the real-time acquisition of IR spectra during hydrothermal reactions. First, H_2O at high pressure and temperature is highly reactive and corrodes most materials. Diamond and 0° sapphire (that is, the optic axis coincides with the *c*-axis of the Al_2O_3 unit cell) are currently the only IR-transparent window materials that withstand the temperature and pressure stress without being chemically degraded. Suitable materials for the main body of the cell in our experience include the metals Au, Ti, and Ta, and the alloys 316-stainless steel (SS), 90/10 Pt−Ir, Inconel, and Hastelloy. Each of these metals has a preferred use that is mostly dictated by the temperature, the nature of the aqueous solution, the location in the reactor, the finances, and the available machining capabilities. Gold foil is excellent for making gaskets,[24,29,44] but gold is rather soft for service as the main body of the cell. Platinum-based alloys and gold make serviceable liners when supported by a stronger material, but they are expensive. 316-SS, Ti, Ta, Inconel, and Hastelloy are less expensive, but the latter three metals require special machine tools. Strong acid and some salts attack 316-SS, but aqueous solutions of many organic compounds were successfully studied below about 620 K. Hot CO_2-H_2O solutions rapidly corroded welded areas of titanium, even when expert care was taken in the welding process.[32] Some CO_2 was retained by the cell which suggests that the mechanism of corrosion may be the formation of $Ti(CO_3)_2$.

Second, a precision flow cell designed for the special considerations of IR spectroscopy is needed. Figure 1 shows a diagram of the 316 SS−sapphire cell.[24] Because the transmission mode is employed, it is desirable to create and maintain a fluid film that has a constant thickness in the range of 20−40 μm at the windows. This was achieved by cutting a slot in the Au foil spacer that accepts the entrance tube, windows, and exit tube.[24,26] The cell body rapidly heats the solution. Fluid mechanics and heat transfer analyses indicate that the plug flow model can be assumed and that the fluid reaches the desired temperature before arriving at the windows.[26] The latter result was verified by calibrating with the vapor−liquid phase boundary of water. From the perspective of achieving maximum information, the best cell incorporated diamond windows and only Pt−Ir alloy and Au in contact with the hot fluid.[26] The resulting band-pass for aqueous solutions and a conventional FTIR spectrometer is about 600−3000 cm^{-1}, but the cell can be fragile and is costly. From the perspective of a long lifetime, the best cells for our purpose are constructed from 316-SS (Figure 1) or Ti with sapphire windows and Au gaskets.[24] These cells are less expensive, but the useful IR band-pass for study of aqueous solutions is limited to about 1700−3000 cm^{-1}. These cells have a surface-to-volume ratio of 20−50 cm^{-1}; however, the design makes it difficult to test for surface effects by varying this number over a wide range. Instead, surface effects can be probed by changing the material of construction.

A third experimental requirement for real-time kinetic measurements at hydrothermal conditions is precise control at all times over the pressure (±1 bar), temperature (±1 K), and flow rate.[24] Because the internal volume of the cell shown in Figure 1 is so small, the flow rate is unusually low (0.01−1 mL/m) which results in residence times of about 1−100 s.

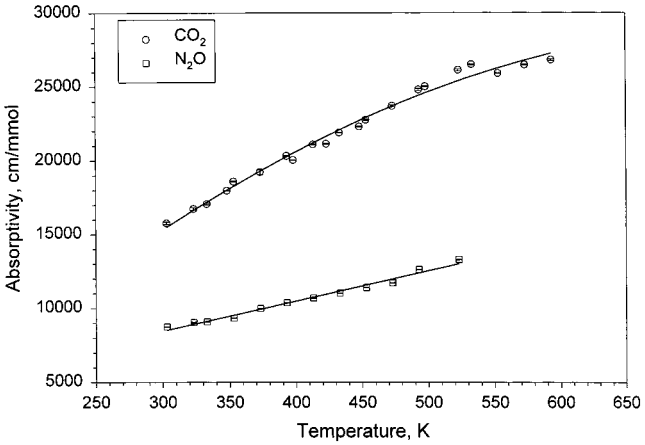

Figure 2. The absorptivity of CO_2 and N_2O in H_2O (275 bar) as a function of temperature.

Variable fluid densities (0.6−1 g/cm^3) exist at the temperatures and pressures used. Therefore, account must be made for the temperature dependence of the fluid density when converting the flow rate to the residence time in the reaction volume. When everything is set up, sealed, and working properly, a Visual Basic program can be devised to control and monitor the operation of the flow apparatus and cell.

Kinetic determinations ideally are based on the concentrations of reactants and products as a function of time at different temperatures. Thus, a fourth experimental problem is the need to know how the absorbance of the chosen IR band changes with temperature at constant concentration. IR spectra of molecules dissolved in H_2O at hydrothermal conditions were not generally known (much less as a function of temperature) when this work began. CO_2 was studied in detail because it is frequently a reaction product and its asymmetric stretch intensely absorbs IR radiation. The prominent P and R rovibrational branches in the gas-phase spectrum of CO_2 disappear in aqueous solution because the water field hinders the rotational degrees of freedom. Only the sharp Q-like vibrational absorption appears, but it broadens asymmetrically as the temperature is raised and begins to resolve just below the critical temperature of H_2O (at 275 bar).[24] In fact, the appearance of the P and R branches with or without the Q branch indicates that an undesirable vapor−liquid-phase separation has occurred in the cell. As shown in Figure 2, the absorptivity of aqueous CO_2 at constant concentration increases by about 70% between 300 and 600 K.[45] The isoelectronic N_2O molecule behaves similarly.[45] This increase in the absorptivity appears to arise from reduced quenching of the induced dipole moment of CO_2 and N_2O by the H_2O field as the temperature is raised.[45] That is, aqueous CO_2 and N_2O become more gaslike as the temperature is raised at constant pressure. These data have practical value in that they are needed to convert the IR absorbance to the absolute concentration at different temperatures.

Results and Discussion

Table 1 summarizes the kinetic information obtained to date with cells of the type shown in Figure 1. The rate constants apply to ≤50% conversion at 275 bar. In some cases the Arrhenius parameters are unreasonable for an uncatalyzed single-step reaction. Corrosion and multiple reactions are apparent in these cases. Furthermore, as illustrated with the malonic acid data in Table 1, the statistical methods used to fit the data and for the error analysis affect the values.[32] Is it worth the effort to obtain these data? So far no radically different reaction mechanisms have been observed, perhaps because the density is liquid water-like. In situ spectral observations using the flow reactor have, however, revealed many reaction details, such as autocatalysis,[26,28,33] competitive reactions at early time,[31,33] reactive intermediates,[26,28] and unusual wall effects.[32,34] The method provides the opportunity to distinguish among possible mechanisms,[28,30,33] and to observe reactor instability caused by an exothermic reaction.[39] Many of these effects would be opaque or at least less directly understandable with ex situ, postreaction methods of determination.

In the following sections, the first reactions described are those of amine-like compounds that form CO_2 and NH_3, mostly through the formation of the cyanate (OCN^-) intermediate. Second, nitrile chemistry is discussed in which NH_3 and in some cases CO_2 are produced. Third, the liberation of CO_2 by carboxylic acids and carboxylate salts is overviewed.

Amine-Like Hydrothermolysis. Scheme 1 concisely summarizes the amine−amide chemistry for which rate constants so far have been spectrally determined at hydrothermal conditions. Starting from the top, the $NH_3-CO_2-H_2O$ equilibrium is prevalent in natural hydrothermal systems and is the end product of many hydrothermal reactions in the absence of a strong oxidizing agent. When derived from aqueous $(NH_4)_2CO_3$, the equilibrium potentially involves the seven species summarized by Scheme 2. The pH and temperature determine the concentrations in a closed cell containing only the liquid phase. As is shown in Figure 3,[39] all of these species can be detected in the 298−448 K range at 275 bar by FT-Raman spectroscopy, except that NH_3 and H_2O are difficult to distinguish. Figure 4 shows the temperature dependence of the IR absorption areas of CO_2, NH_4^+, and HCO_3^- at the same conditions as employed in Figure 3.[24] Flow and stopped-flow data were recorded to verify that equilibrium is attained in the flow mode. As a result of the lower dielectric constant of H_2O at higher temperature, charged species become the less favored form of the molecules. Hence, the equilibrium in Scheme 2 shifts from the right-hand side to the left-hand side as the temperature is raised. The temperature and $[H^+]$ dependence of Scheme 2 must be taken into account when the CO_2 concentration is used to indicate the reaction rate. This is because the total amount of CO_2 produced is not necessarily reflected by the absorption intensity of CO_2 alone, especially when the solution is basic. Although $NH_3-CO_2-H_2O$ is buffered, different amounts of H^+ or OH^- change the relative ratios of CO_2, HCO_3^- and CO_3^{2-}.

Moving down in Scheme 1, the hydrothermolysis of MOCN salts (M = Na^+, NH_4^+) as a function of the pH is a process common to many amine and amide reaction networks. A detailed kinetics study was therefore undertaken for NaOCN at pH = 3.94−10.5.[35] The three reactions shown in Scheme 3 are simple variations of one another, but the rates of each were needed to model the process completely. The rate constant k_1 reflects pseudo first-order hydrolysis at the natural pH (10.5) of aqueous NaOCN. The rate, however, increases with time because the NH_3 product has an autocatalytic effect. This is accounted for by the rate constant k_2. Mechanistically, the higher concentration of NH_3 may increase the amount of carbamate ($NH_2CO_2^-$) in Scheme 2, and thereby provides another pathway to the products. The reaction rate at acidic conditions (k_3) is even greater, which leads to the overall trend: $k_3 > k_2 > k_1$.

The cyanate salt NH_4OCN is of interest as an intermediate in the hydrothermolysis of urea in Scheme 1.[24,26] The interconversion of ammonium cyanate and urea is a landmark of chemical discovery[46] and continues to have practical importance.[47] Figure 5 shows IR spectra for 1.05 *m* urea at several

TABLE 1: Kinetic Constants for Reactions of the Compounds Listed at Hydrothermal Conditions (275 bar) as Measured in Real Time by IR Spectroscopy

compound	cell material	[mol/kg]	E_a, kJ/mol	ln(A, s^{-1})	T, K[a]	$\Delta S^{\ddagger}$, J/mol*K	ref
			Acids				
HCO_2H	316-SS	1	113 ± 10	20 ± 2	553−603	−108	32
HCO_2H	90/10 Pt−Ir	1	120 ± 23	21 ± 5	573−603	−84	32
HCO_2H	Ti	1	82 ± 12	11 ± 2	563−593	−167	32
$NCCH_2CO_2H$	316-SS	0.25	173 ± 2	40 ± 1	433−493	74	34
$NCCH_2CO_2H$	Ti	0.25	149 ± 10	33 ± 3	423−473	18	34
CF_3CO_2H	316-SS	0.25	192 ± 5	43 ± 1	453−523	96	34
CF_3CO_2H	Ti	0.25	151 ± 11	32 ± 3	453−523	55	34
CCl_3CO_2H	316-SS	0.25	184 ± 9	53 ± 3	383−423	190	34
CCl_3CO_2H	Ti	0.25	300 ± 40	86 ± 12	383−423	460	34
$CF_3CH_2CO_2H$	316-SS	0.25	84 ± 6	16 ± 2	453−523	−124	34
$CF_3CH_2CO_2H$	Ti	0.25	79 ± 8	15 ± 2	463−503	−134	34
$CH_3C(O)CO_2H$	316-SS	0.25	75 ± 7	13 ± 2	473−513	−150	34
$CH_3C(O)CO_2H$	Ti	0.25	32	2.1	473−513	−240	34
$NH_2C(O)CH_2CO_2H$	316-SS	0.25	146 ± 9	37 ± 3	413−473	48	34
$NH_2C(O)CH_2CO_2H$	Ti	0.25	147 ± 3	38 ± 1	413−473	58	34
$HO_2CCH_2CO_2H$	316-SS	1.07	126 ± 2	31 ± 1	393−483	4	27
$HO_2CCH_2CO_2H$	90/10 Pt−Ir	1	96 ± 3	23 ± 1	463−503	−78	27
$HO_2CCH_2CO_2H$	Ti	1	121 ± 7	30 ± 1	453−473	−6	34
$HO_2CCH_2CO_2H$[c]	316-SS	1.07	90 ± 31	21.4 ± 8	393−483	−78	32
$HO_2CCH_2CO_2H$[c]	90/10 Pt−Ir	1.07	91.5 ± 5	21.7 ± 1	393−483	−78	32
$HO_2CCH_2CO_2H$[c]	Ti	1.07	93 ± 8	21.4 ± 2	393−483	−78	32
			Carboxylates				
HCO_2Na	316-SS	1	100 ± 1	16 ± 1	553−603	−150	32
HCO_2Na	90/10 Pt−Ir	1	31 ± 8	2.3 ± 1.5	573−593	−240	32
HCO_2Na	Ti	1	No rxn				32
$NCCH_2CO_2Na$	316-SS	0.25	120 ± 3	28 ± 1	413−473	−26	34
$NCCH_2CO_2Na$	Ti	0.25	103 ± 3	23 ± 6	433−503	−70	34
CF_3CO_2Na	316-SS	0.25	178 ± 14	40 ± 5	463−513	72	34
CF_3CO_2Na	Ti	0.25	128 ± 11	26 ± 3	463−513	−38	34
CCl_3CO_2Na	316-SS	0.25	66 ± 5	16 ± 1	383−423	−120	34
CCl_3CO_2Na	Ti	0.25	68 ± 8	17 ± 2	383−433	−110	34
$CF_3CH_2CO_2Na$	316-SS	0.25	62 ± 3	13 ± 1	463−533	−150	34
$CH_3C(O)CO_2Na$	316-SS	0.25	64	10	473−513	−174	34
$NH_2C(O)CH_2CO_2Na$	316-SS	0.25	81 ± 5	15 ± 1	443−503	−130	34
$NH_2C(O)CH_2CO_2Na$	Ti	0.25	46 ± 4	6 ± 1	443−503	−200	34
$HO_2CCH_2CO_2Na$	316-SS	1.07	117 ± 5	28 ± 1	393−483	−21	34
			Amines and Amides				
$(NH_2)_2CO$	316-SS	1.05	88	18	473−573	−112	24
$(NH_2)_2CO$	90/10 Pt−Ir	1.05	83 ± 4	17 ± 1	473−573	−112	26
NH_2CN	316-SS	0.5	116 ± 12	28 ± 3	403−453	−27	31
$2NH_2CN$	316-SS	0.5	96 ± 6	31 ± 2[b]	403−453	−2	31
$(NH_2)_2CNCN$	316-SS	0.25	73 ± 3	12 ± 1	473−543	−156	31
$(NH_2)_2CNC(O)NH_2$	316-SS	0.25	90 ± 2	19 ± 1	473−543	−103	31
$NH_2C(O)N_2H_4^+$	Ti	0.25	109 ± 2	26 ± 0.5	413−443	−41	33
$NH_2C(NH)N_2H_4^+$ (pH = 2)	Ti	1	91 ± 11	15 ± 3	483−503	−133	33
$NH_2C(NH)N_2H_4^+$ (pH = 5.6)	Ti	1	47 ± 4	23 ± 1[b]	423−533	−64	33
$(NH_2NH)_2CO$	90/10 Pt−Ir	1.07	88 ± 1	18	503−543	−108	28
			Cyanates				
NH_4OCN	316-SS	0.5	59	17[b]	473−573	−117	24
NH_4OCN	90/10 Pt−Ir	0.5	66 ± 6	20 ± 1[b]	473−573	−92	26
NH_4SCN	316-SS	1	113 ± 11	21 ± 2[b]	543−573	−84	30
NaOCN (pH = 9)	Ti	0.25	81 ± 2	18 ± 0.5	383−433	−105	33
NaOCN (autocatal.)	Ti	0.25	75 ± 10	20 ± 3[b]	393−433	−93	33
HOCN (pH = 6)	Ti	0.25	30 ± 8.5	7 ± 2	383−423	−196	33
			Nitriles				
CH_3CN (pH = 0.5)	Ti	1	127 ± 3	28 ± 1[b]	473−533	−25	35
C_2H_5CN (pH = 0.5)	Ti	1	90 ± 1	20 ± 0.4[b]	423−533	−92	35
$(CH_3)_2CHCN$ (pH = 0.5)	Ti	0.5	82 ± 4	17.8 ± 1[b]	443−533	−109	35
HO_2CCH_2CN (pH = 1.5)	Ti	1	145 ± 18	23 ± 1[b]	423−503	23	35
			Misc.				
$[NH_3OH]NO_3$	316-SS	0.2	103 ± 21	21 ± 5	463−523	−80	29
OCS	316-SS	0.23	44 ± 5	13 ± 1	393−423	−150	30

[a] Entropy of activation calculated at the approximate midpoint of the temperature range. [b] Units are kg mol^{-1} s^{-1}. [c] Different statistical method used.

residence times when the Pt−Ir−diamond cell is set at 513 K and 275 bar. Several features are noteworthy. First, the very high S/N permits the line shapes to be fitted accurately with Voigt functions. Second, the spectral baseline reveals the presence of an interference fringe pattern, which can be used to determine the path length of the cell. The path length was found to be constant in the temperature range of our studies (373−623 K). Finally, the relative areas of the CO_2, HCO_3^-,

SCHEME 1

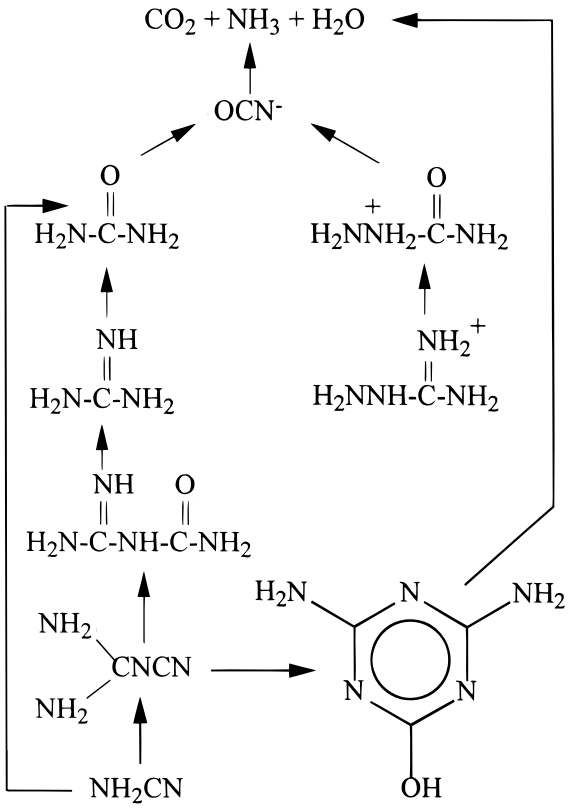

SCHEME 2

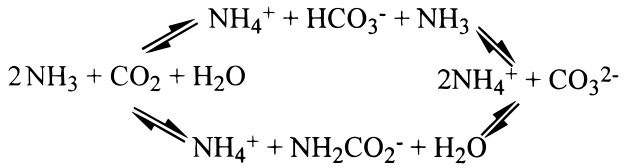

and CO_3^{2-} bands provide the pH once the equilibrium equation is solved. The availability of an in situ method to measure pH is valuable when modeling hydrothermal reactions. Returning to Figure 5, the concentrations of the species shown in Scheme 4 can be matched quantitatively below 50% conversion by iteratively solving for the rate constants. There is spectral evidence, however, that Scheme 4 equilibrates at greater extents of conversion.[24,26] Hence, urea is produced from aqueous NH_3 and CO_2 at hydrothermal conditions, which may be important for synthesis of energy-richer molecules at geothermal vents.

The rate of conversion of NH_4OCN to NH_3 and CO_2 is faster than that of NaOCN at the same temperature. We also determined the kinetics and pathway of hydrothermolysis of NH_4SCN for comparison with NH_4OCN.[30] SCN^- is present in coke-oven wastewater[48,49] and is considered to be nonbiodegradable.[50] As such, its destruction by hydrothermal methods may be of interest. SCN^- forms OCS, rather than OCN^-, as an intermediate, which was proven by real-time IR spectroscopy. A separate kinetics study of OCS revealed rapid hydrolytic conversion to CO_2 and H_2S, and therefore OCS is not detected in the reaction of NH_4SCN.[30] The rate of hydrothermolysis of NH_4SCN is about 1/3000 that of NH_4OCN at 543 K. This difference originates from the fact that the S−C bond is less polar than the O−C bond, which makes nucleophilic attack at C less favored in SCN^-.

Returning to Scheme 1, the kinetics data for OCN^- at different values of the initial pH (296 K) can be used to develop

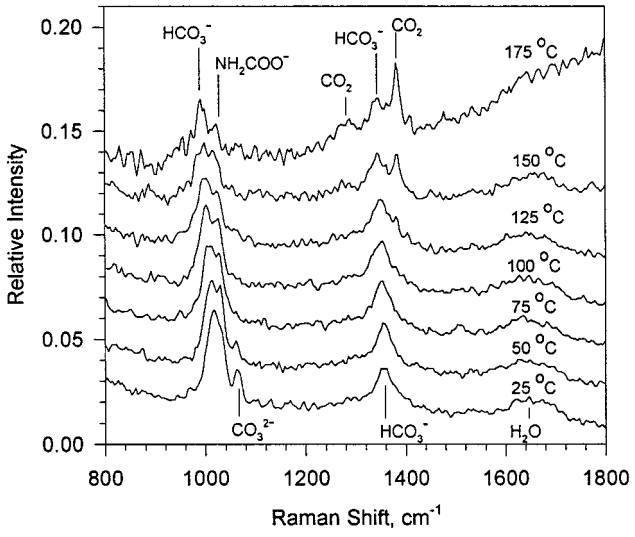

Figure 3. FT-Raman spectra of 1.2 *m* $(NH_4)_2CO_3$ at 275 bar as a function of temperature showing the components of Scheme 2.

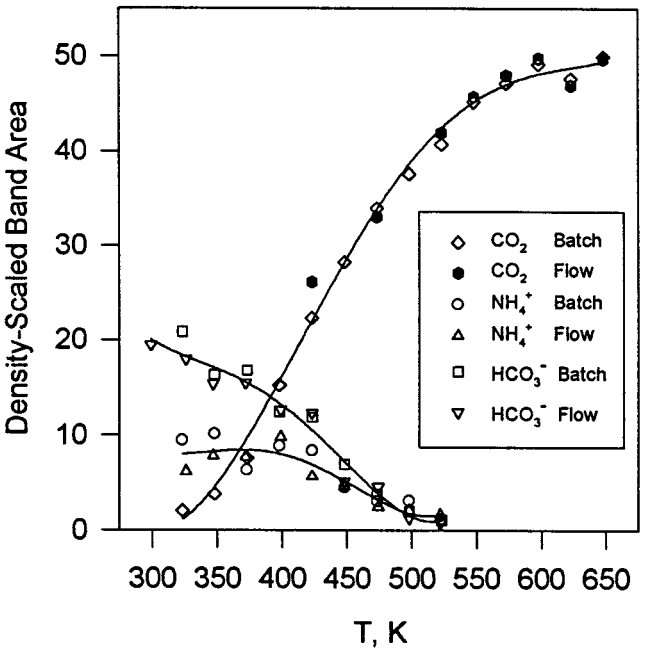

Figure 4. The band areas of the species shown from the IR spectrum of 0.1 *m* $(NH_4)_2CO_3$ at 275 bar as a function of temperature. The charged species become less favored at higher temperature.

SCHEME 3

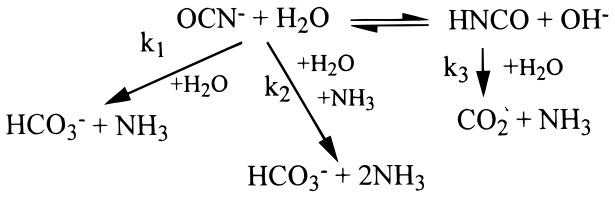

the hydrothermolysis pathways of the hydraza-containing compounds semicarbazide and aminoguanidine.[33] Weakly basic semicarbazide was studied at pH values of 2.1 and 5.7 by adding HNO_3, and the reaction rate is lower at higher pH. In addition to aqueous CO_2 and NH_3 discussed above, N_2H_4 is produced. N_2H_4 is relatively unreactive at the conditions of the measurements;[37] however, the decomposition rate of N_2H_4 in the presence of HNO_3 depends on the reactor surface, being faster on 316-SS than on Ti.[33] The availability of the hydrothermolysis

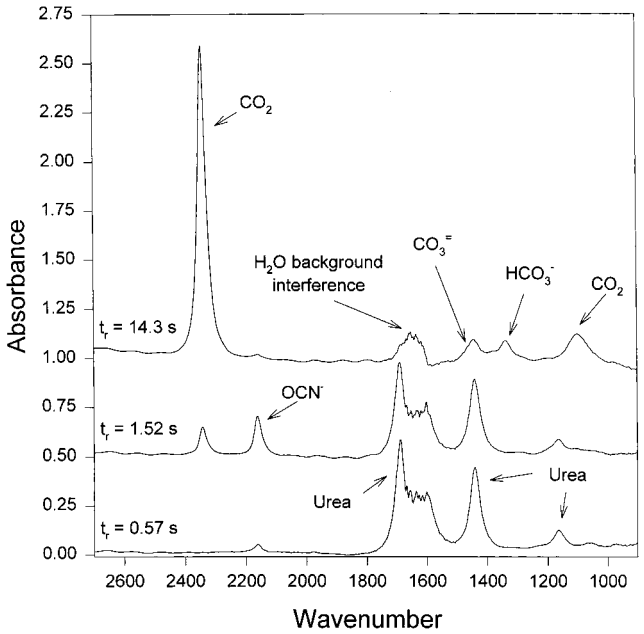

Figure 5. IR spectra of 1.05 *m* $(NH_2)_2CO$ at 513 K and 275 bar showing the reactants intermediate and products. The diamond Pt−Ir cell was used.

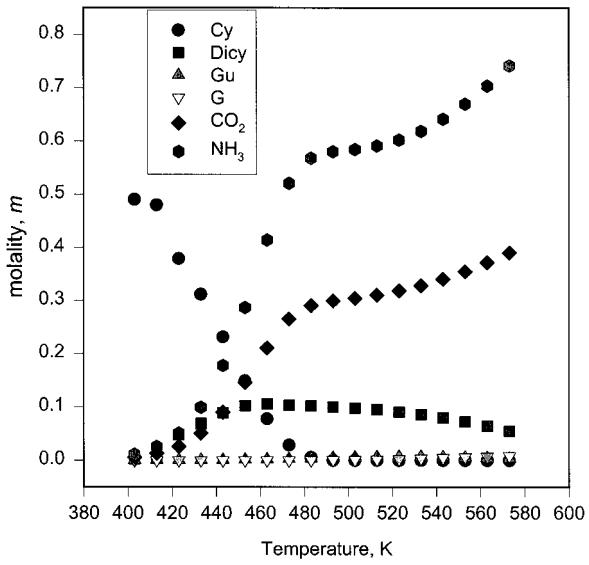

Figure 6. The concentrations of the species from cyanamide (Cy) (Scheme 1) after 10 s of reaction time at the temperatures shown and 275 bar. Dicy = dicyandiamide, Gu = guanyl urea, G = guanidine.

SCHEME 4

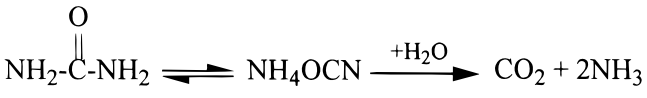

SCHEME 5

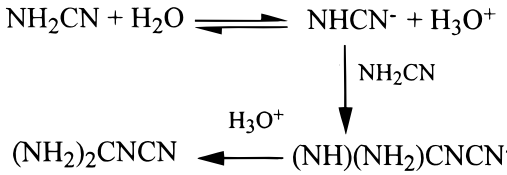

kinetics for semicarbazide as a function of pH permits the kinetics of aminoguanidine to be determined. Aminoguanidine is more basic than semicarbazide, and its kinetics were determined at pH = 1.6, 2.4, and 5.6. In contrast to semicarbazide the rate at higher pH is greater than at lower pH. An explanation is that the aminoguanidinium cation converts more rapidly to semicarbazide in the presence of OH^- because neutral aminoguanidine is more reactive.[33] Most of the rates in this reaction network extrapolate reasonably well to those in the normal liquid range of H_2O which suggests that the reaction mechanisms are similar at both conditions.

The hydrothermolysis kinetics of carbohydrazide $(NH_2NH)_2CO$[28] may be useful because carbohydrazide is used as an antioxidant to reduce corrosion in steam boilers.[51,52] Carbohydrazide hydrolyzes to CO_2 and N_2H_4 through a putative hydrazacarboxylate intermediate ($NH_2NHCO_2^-$) which is analogous to the carbamate intermediate mentioned above.

The availability of the urea−cyanate conversion kinetics also enables the kinetics of the hydrothermolysis pathways for NH_2CN and guanidine to be determined as summarized in Scheme 1. While the guanidine kinetics reflect straightforward hydrolysis to urea,[26] cyanamide reacts by the most complex pathway encountered to date in our work.[31] The effort devoted to elucidate the NH_2CN reaction network seemed justified in the context of the chemical evolution hypothesis of Calvin,[53,54] and the fact that cyanamide has widespread application in industrial processes. NH_2CN is observed in interstellar space[55] and readily dimerizes to dicyandiamide $(NH_2)_2CNCN$. Calvin's group showed that both are formed when a mixture of NH_3, HCN, CH_4, and H_2O is exposed to e-beam radiation.[54] The resulting dicyandiamide acts as a dehydration coupling agent that is able to link glucose and adenosine to H_3PO_4 and produce glucose-6-phosphate and adenosine-5′-phosphate, respectively.[53] Therefore, the hydrothermal reactivity of NH_2CN and $(NH_2)_2$-CNCN may be of interest because this is key information before considering these molecules as possible active agents at hydrothermal conditions. Moreover, this information is needed if industrial waste streams containing these molecules are treated by hydrothermally based methods of destruction.

Using Scheme 1 as the outline, Raman spectroscopy proved that the hydrothermolysis of NH_2CN initially forms urea,[32] which subsequently liberates CO_2 and NH_3 at a rate specified by the kinetics discussed above. This reaction increases the pH and shifts the ionization equilibrium of NH_2CN (Scheme 5) toward the right-hand side. The species in this equilibrium react with one another and produce neutral dicyandiamide. NH_2CN, $(NH_2)_2CNCN$, and CO_2 can be quantified simultaneously as a function of time and temperature from the IR spectrum. Hence a complete kinetic model can be parametrized for the pH-dependent, dual reaction of NH_2CN as a function of temperature.

A dual hydrothermolysis pathway also exists for dicyandiamide.[32] Hydrolysis forms guanyl urea, which cascades to CO_2 and NH_3 via the steps shown in Scheme 1. $(NH_2)_2CNCN$ also reacts with CO_2 and NH_3 to produce the *s*-triazine derivative ammeline[32] along with the other three *s*-triazine derivatives which together represent all of the combinations of NH_2 and OH substituents (melamine, ammelide, and cyanuric acid).[56] These cyclic azines appear to stick to the reactor wall so that kinetic information could not be obtained for this step. By conducting separate hydrothermal experiments, however, each *s*-triazine derivative was determined to hydrothermolyze to CO_2 and NH_3 at higher temperature and/or longer time.[32,56] Thus, NH_2CN eventually decomposes to CO_2 and NH_3 but it does so by several pathways and not before synthesizing larger molecules.

This study of NH_2CN, when summarized as in Figure 6, answers the question of whether dicyandiamide has a sufficient lifetime in the presence of NH_3 and CO_2 at hydrothermal

SCHEME 6

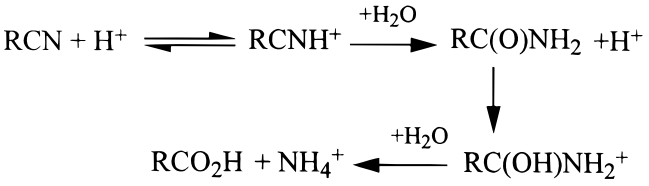

conditions to play a role in chemical evolution. Based on the complete kinetic model, the concentrations of all species can be calculated at plausible values of the residence time (e.g., 10 s) for a series of temperatures that are typical of the shear layer of a geothermal vent. Figure 6 shows that a reasonable concentration of dicyandiamide exists even at the 573 K limit of this determination.

Nitrile Hydrothermolysis. The hydrothermolysis chemistry of alkyl nitriles is somewhat related to the processes of the amine-like compounds discussed above. One popular hypothesis is that the Strecker synthesis or a closely related process may have provided smooth access to α-amino- and α-hydroxyalkyl carboxylate molecules that are necessary for living systems.[57−60] More specifically, aldehydes and ketones react with NH_3 and HCN to form α-amino- and α-hydroxyalkyl nitriles which then hydrolyze to the corresponding substituted carboxylic acids. Hence the hydrothermolysis of alkyl nitriles may be of interest in this area. Furthermore, the nitrile group finds widespread application in the production of commercial products and as a result may show up in aqueous waste streams that could be hydrothermally denatured. Kinetic measurements of hydrothermolysis of several alkyl nitrile compounds were therefore undertaken by IR spectroscopy.[34]

Alkyl nitriles are well-known to hydrolyze more rapidly in the presence of acid.[61] After probing a number of reaction variables, the kinetics of the reactions shown in Scheme 6 described the process, although only the disappearance of the nitrile absorbance was followed by IR spectroscopy. Additional support for Scheme 6 came from the pH dependence of the reaction and the curvature of the RCN concentration profile with time. The resulting Arrhenius parameters are given in Table 1. The carboxylic acid product of hydrothermolysis decarboxylates if the temperature is high enough, and so the $CO_2-NH_3-H_2O$ equilibrium mixture can form as discussed above. A conclusion from this work is that the rate of hydrothermolysis of simple alkyl nitriles is relatively low at the residence times and temperatures (473−623 K) typical of the shear layer of a geothermal vent. The presence of acid greatly increases the rate. Nitrile hydrothermolysis also may be affected by other substituents attached to the alkyl group. A role of such a substituent is discussed below in the decarboxylation of cyanoacetic acid.

Carboxylate Hydrothermolysis. Given the prevalence of carboxylic acids RCO_2H and their salts $RCO_2^-M^+$ in natural and industrial processes, considerable attention was given to determining their kinetics of decarboxylation. This reaction is believed to be a major factor in the relative concentrations of organic acids in subsurface water, such as brine[62] and geothermal vents.[63] If carboxylic acids are not initially present in an aqueous waste stream being subjected to remediation by supercritical water oxidation or wet air oxidation, then they can form as intermediates in the oxidation process. As such, the sequential degradation of the organic components may take place through successive oxidation and decarboxylation reactions.

Some of the factors that influence the rate of decarboxylation of RCO_2H have been reviewed by Bell and Palmer for several R groups.[64] One method to classify carboxylic acids is by the

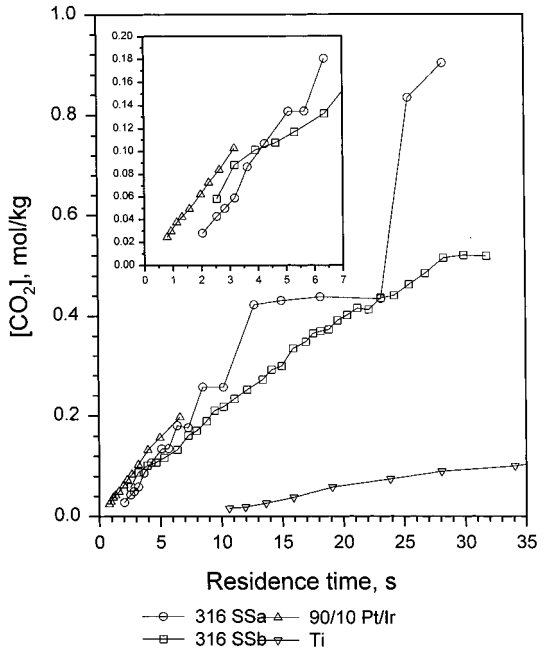

Figure 7. The CO_2 concentration versus time produced by 1.0 m HCO_2H at 583 K and 275 bar in four types of cell materials.

Hammett or Taft electronic characteristics of the R group: electron-donating, electron-neutral, electron-withdrawing. Another method might be by the surface on which the acid reacts. An important question is the comparative roles played by the characteristics of R vs the nascent heterogeneous surfaces. Acetic acid, for which the electron-donating CH_3 group strengthens the C−C-bond, is the most stable and inert of the aliphatic acids. This fact contributes to its high concentration in brine. On the other hand, the rate of decomposition of CH_3CO_2H (possibly to $CH_4 + CO_2$) is a strong function of the substrate surface, e.g., $t_{1/2}$ is about 10^{14} times longer on SS than on Ti at 373 K.[65] Because of their low reactivity at the residence times and temperatures available in the flow reactor, our laboratory contributed nothing new to the kinetics of acids having electron-donating R groups. Instead, reliance was placed on the work just cited that electron-donating R groups impart stability, but that the reactivity can be strongly affected by heterogeneous surfaces.

Formic acid has R = H which is electronically neutral on the Hammett−Taft scale. Only the decomposition channel to $CO_2 + H_2$ was observed by IR spectroscopy at hydrothermal conditions,[32] although a 10% contribution from the $CO + H_2O$ channel was detected by GC.[66] This difference may simply result from the low IR absorptivity of CO which makes its detection difficult. The water-gas shift reaction may also contribute to the CO_2/CO ratio.[67] Both the appearance of CO_2 at 2343 cm^{-1} and the disappearance of the C−H stretch at 2940 cm^{-1} can provide the decarboxylation rate, but CO_2 is a more useful because of its much greater IR absorptivity. Formic acid, however, exhibited interesting and perplexing results in flow cells constructed from different materials.[32] Four cells having the same design but constructed from Pt−Ir, Ti, and two batches of 316-SS were compared. As shown in Figure 7, different batches of 316-SS exhibited both steadily increasing and stepped rates of generation of CO_2, whereas Pt−Ir and Ti exhibited steadily increasing, but different, rates. The rate on Ti was lower than that on 316-SS or Pt−Ir by a factor of about 10 at 583 K. The stepped concentration behavior was reproducible in the SS cell where it occurred but the origin is unclear. Curiously,

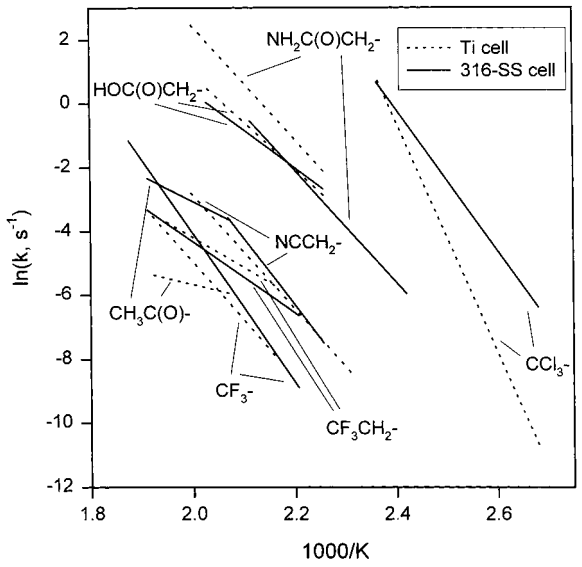

Figure 8. An Arrhenius plot comparing the rates of decarboxylation of RCO_2H (R is identified on the plot) in 316-SS and Ti cells at 275 bar.

however, HCO_2H behaves similarly on Ni(110) at ultrahigh vacuum conditions.[68] The dependence of the rate on the cell material at hydrothermal conditions suggests that a significant wall effect exists when R = H, but the effect is not nearly as large as that cited above for R = CH_3.

The main effort in this laboratory was devoted to measuring the decarboxylation kinetics of RCO_2H when R is electron withdrawing.[34] The initial step is formation of RH + CO_2. Table 1 contains a summary of the kinetic parameters obtained for the acids and the corresponding sodium carboxylate salts with 316-SS and Ti cells. The Arrhenius parameters for R = CCl_3 and $CH_3C(O)$ are rather unrealistic, but their reactions are complicated by corrosion of the 316-SS cell by the chloro derivative and further reactions of the RH product in both cases. Figure 8 is a composite Arrhenius plot comparing the behavior of each acid in 316 SS and Ti. With the exception of R = CCl_3 and $CH_3C(O)$, the rates are rather similar in both cells. Overall the effect of changing R is much greater than the effect of changing the metal of construction. This observation, when combined with the fact that the temperature range needed for these reactions (373−533 K) is lower than that needed when R = H or CH_3, suggests that the homogeneous pathway to decarboxylation is more prevalent for these acids than is the heterogeneous pathway. Therefore, we conclude that the balance of the roles of homogeneous and heterogeneous pathways depends at least in part on the strength of the R−CO_2H bond. Acids with the weakened R−C bond decarboxylate without major catalytic assistance from the surface, whereas decarboxylation of acids with a stronger R−C bond benefits from surface assistance. That is, the decarboxylation rate of acids having electron-donating R groups is more sensitive to the material of construction of the reactor than acids with electron-withdrawing R groups.

The solvent apparently plays a greater role in the decarboxylation of carboxylate anions RCO_2^- than the acids, as the reaction stoichiometry suggests. Hence, a more ordered transi-

$$RCO_2H \rightarrow RH + CO_2$$

$$RCO_2^- + H_2O \rightarrow RH + CO_2 + OH^-$$

tion state is expected as a result of both electrostriction and the fact that H_2O is a required reactant. Hence $\Delta S^{\ddagger}$ should be and is lower than that of the corresponding acid in almost every case (Table 1). Also, the reaction rate tends to be greater for the anion than the acid when R does not possess the keto group, whereas the reverse is found for keto-containing R groups. This result may be explained by the added resonance stabilization provided to the anion when R contains the keto group.

SCHEME 7

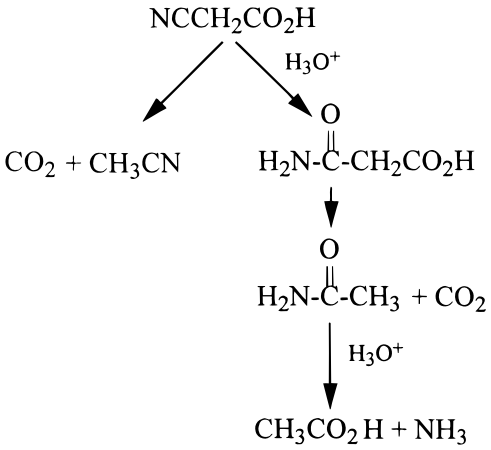

A somewhat more complex situation arises when two hydrothermally reactive functional groups are present in the same molecule. An example is the hydrothermolysis of cyanoacetic acid at 433−533 K with and without the presence of a strong acid.[34] As noted above, the rate of hydrothermolysis of the nitrile group depends on pH and is faster at lower pH. On the other hand, the decarboxylation rate of the acid exhibits little sensitivity to the pH at acidic conditions. Thus, without added acid cyanoacetic acid decarboxylates straightforwardly according to Scheme 7. The system is spectroscopically over determined because the nitrile reactant and the CO_2 and CH_3CN products can all be measured. When a strong acid is added, however, a different set of products appears. In this case the nitrile group preferentially hydrothermolyzes giving NH_3, CO_2, and CH_3CO_2H as the final products.

Concluding Remarks

Obtaining high-quality, real-time, IR spectral measurements at hydrothermal conditions requires considerable effort given the harsh conditions. On the other hand, insights are gained that may not be available without directly observing the reaction in progress. Experimental difficulties aside, we occasionally encountered wildly erratic results that may originate from a change in the surface characteristics of the metal reactor. This hypothesis suggests that a promising avenue of future research is to investigate the interfacial metal−fluid characteristics at hydrothermal conditions. It is likely that chemical events occur at this interface that are just as interesting as those found at high vacuum.[68] It would be worthwhile to employ other spectral techniques, especially Raman spectroscopy, along with other ranges of pressure, temperature, and concentration in an attempt to discover reaction phenomena different from those observed so far.

A problem facing every researcher chancing into the field of hydrothermal reactions is the lack of a general "pH meter" to keep track of subtle changes in the pH. Several excellent specialized methods are available including the relative CO_2−HCO_3^-−CO_3^{2-} band areas in the IR spectrum that were shown in Figure 5. As noted several times in this article, however, a shift in the pH may change the mechanism. Another problem

is that spontaneously exothermic reactions are difficult to study with a flow reactor where it is desirable to maintain a constant pressure, temperature, and flow rate. The behavior of reactive nitrate salts is an example[29,39,69] not discussed in this article. Spontaneously exothermic reactions can produce reactor instability or much more serious consequences if they are not anticipated.

A reality of most industrial and all-natural hydrothermal processes is that salts are present during the reaction. Thus, a territory of opportunity is to investigate the effect of salts and metal ions on the rates of the reactions discussed herein. Work of this type is currently underway in our laboratory.

Hydrothermal chemistry is one of those wonderful areas with profound implications, practical applications, and fundamental questions. Like every interesting field of research, it has difficult problems to overcome and perplexing observations that need to be understood, but when success is achieved it seems well worth the great effort.

Acknowledgment. Drs. Alec Belsky, Matthew Kieke, Patrick Maiella, and Joseph Schoppelrei conducted the work described in this article as part of their doctoral dissertation requirements. Support for the research has mostly come from the Army Research Office (DAAL03-92-G-0174 and DAAG55-98-1-0253) and the National Science Foundation (CHE-9807370).

References and Notes

(1) Spooner, E. T. C.; Bray, C. T. *Nature*, **1977**, *266*, 808.
(2) Spiess, F. N., et al. *Science* **1980**, *207*, 1421.
(3) *Hydrothermal Processes at Sea Floor Spreading Centers*; Rona, P. A., Bostrom, K., Laubier, L., Smith, K.L., Eds.; Plenum: New York, 1984.
(4) Haymon, R. M.; Macdonald, K. C. *Am. Sci.* **1985**, *73*, 441.
(5) Lundegard, P. D.; and Kharaka, Y. K. In *Chemical Modeling of Aqueous Systems II*; (Melchior, D. C., Bassett, R. L., Eds.; *ACS Symp. Ser. 416*, **1990**, p 169.
(6) Shock, E. L. *Geochim. Cosmochim. Acta* **1993**, *57*, 3341.
(7) *Organic Acids in Geological Processes*; Pittman, E. D., Lewan, M. D., Eds.; Springer-Verlag: Berlin, 1994.
(8) Shock, E. L. *Geochim. Cosmochim. Acta*, **1990**, *54*, 1175.
(9) Schulte, M. D.; Shock, E. L. *Geochim. Cosmochim. Acta* **1993**, *57*, 3735.
(10) Shock, E. L.; Koretsky, C. M. *Geochim. Cosmochim. Acta* **1995**, *59*, 1497.
(11) Lutz, R. A.; Shank, T. M.; Fornari, D. J.; Haymon, R. M.; Lilley, M. D.; Von Damm, K. L.; Desbruyeres, D. *Nature* **1994**, *371*, 663.
(12) Shock, E. L. *Origins Life Evol. Biosphere*, **1992**, *22*, 67.
(13) Wächtershäuser, G. *Prog. Biophys. Mol. Biol.* **1992**, *57*, 75.
(14) Huber, C.; Wächtershäuser, G. *Science* **1997**, *276*, 245.
(15) Shaw, R. W.; Brill, T. B.; Clifford, A. A.; Eckert, C. A.; Franck, E. U. *Chem. Eng. News* **1991**, December 23, 26.
(16) Tester, J. W.; Holgate, H. R.; Armellini, F. J.; Webley, P. A.; Killilea, W. R.; Hong, G. T.; Barner, H. E. In *Emerging Technology in Hazardous Waste Management III*; Tedder, D. W., Pohland, F. G., Eds.; *ACS Sym. Ser. 517* **1993**, 35.
(17) Savage, P. E. *Chem. Rev.* **1999**, *99*.
(18) Katritzky, A. R.; Allin, S. M.; Siskin, M. *Acc. Chem. Res.* **1996**, *29*, 399.
(19) Mishra, V.; Mahajani, V. V.; Joshi, J. B. *Ind. Eng. Chem. Res.* **1995**, *34*, 2.
(20) Savage, P. E.; Gopalan, S.; Mizan, T. I.; Martino, C. J.; Brock, E. E. *AIChE J.* **1995**, *41*, 1723.
(21) Ding, Z. Y.; Frisch, M. A.; Li, L.; Gloyna, E. F. *Ind. Eng. Chem. Res.* **1996**, *35*, 3257.
(22) Nematsu, M.; Franck, E. U. *J. Phys. Chem. Ref. Data* **1980**, *9*, 1291.
(23) Marshall, W. L.; Franck, E. U. *J. Phys. Chem. Ref. Data* **1981**, *10*, 295.
(24) Kieke, M. L.; Schoppelrei, J. W.; Brill, T. B. *J. Phys. Chem.* **1996**, *100*, 7455.
(25) Maiella, P. G.; Brill, T. B. *Inorg. Chem.* **1996**, *50*, 829.
(26) Schoppelrei, J. W.; Kieke, M. L.; Wang, X.; Klein, M. T.; Brill, T. B. *J. Phys. Chem.* **1996**, *100*, 14343.
(27) Maiella, P. G.; Brill, T. B. *J. Phys. Chem.* **1996**, *100*, 14352.
(28) Schoppelrei, J. W.; Brill, T. B. *J. Phys. Chem. A* **1997**, *101*, 2297.
(29) Schoppelrei, J. W.; Brill, T. B. *J. Phys. Chem. A* **1997**, *101*, 8593.
(30) Maiella, P. G.; Brill, T. B. *Inorg. Chem.* **1998**, *37*, 454.
(31) Belsky, A. J.; Brill, T. B. *J. Phys. Chem. A* **1998**, *102*, 4509.
(32) Maiella, P. G.; Brill, T. B. *J. Phys. Chem. A* **1998**, *102*, 5886.
(33) Belsky, A. J.; Brill, T. B. *J. Phys. Chem. A.* **1999**, *103*, 3006.
(34) Belsky, A. J.; Maiella, P. G.; Brill, T. B. *J. Phys. Chem. A.* **1999**, *103*, 4253.
(35) Belsky, A. J.; Brill, T. B. *J. Phys. Chem. A.* **1999**, *103*, 7826.
(36) Buback, M. *Angew. Chem.* **1991**, *30*, 641.
(37) Masten, D. A.; Foy, B. R.; Harradine, D. M.; Dyer, R. B. *J. Phys. Chem.* **1993**, *97*, 8557.
(38) Myrick, M. L.; Kohs, J.; Parsons, E.; Chike, K.; Lovelace, M.; Scrivens, W.; Holliday, R.; Williams, M. J. *Raman Spectrosc.* **1994**, *25*, 59.
(39) Schoppelrei, J. W.; Kieke, M. L.; Brill, T. B. *J. Phys. Chem.* **1996**, *100*, 7463.
(40) Bell, W. C.; Boohsh, K. S.; Myrick, M. L. *Anal. Chem.* **1998**, *70*, 332.
(41) Croiset, E.; Rice, S. F. *Ind. Eng. Chem. Res.* **1998**, *70*, 1755.
(42) Bennett, G.; Johnston, K. P. *J. Phys. Chem.* **1994**, *98*, 441.
(43) Terry, J. L.; Fox, M. A. *J. Phys. Chem. A.* **1998**, *102*, 3705.
(44) Spohn, P. D.; Brill, T. B. *Appl. Spectrosc.* **1987**, *41*, 1152.
(45) Maiella, P. G.; Brill, T. B. *Appl. Spectrosc.* **1999**, *53*, 351.
(46) Wöhler, F. *Ann. Phys. Chemie* **1829**, *75*, 619.
(47) Schaker, P. M.; Colson, J.; Higgens, S.; Dietz, E.; Thielen, D.; Anspach, B.; Brauer, J. *Am. Lab*, **1999**, August 13.
(48) Chowdhury, A. K.; Copa, W. M. *Ind. Chem. Eng.* **1986**, *28*, 3.
(49) Copa, W. M.; Gitchel, W. B. *Standard Handbook of Hazardous Waste Treatment and Disposal*; Freeman, W. H., Ed.; McGraw-Hill: New York, 1989; Sect. 8.8.
(50) Horak, O. *Chem. Ing. Tech.*, **1990**, *6*, 555.
(51) Akolzin, A. P.; Klochkova, B. V. G.; Balsbanov, A. E. *Tepioenergetika* (*Moscow*) **1988**, 61 (CA 109: 196843p).
(52) Van der Wissel, J. T. M. *Polytech. Tijdschr. Proscestech.* **1991**, *46*, 40.
(53) Steinman, G.; Lemmon, R. M.; Calvin, M. *Proc. Natl. Acad. Sci. U.S.A.*, **1964**, *2*, 27.
(54) Schimpl, A.; Lemmon, R. M.; Calvin, M. *Science*, **1965**, *147*, 49.
(55) Turner, B. E.; Kislyakov, A. G.; Liszt, H. S.; Kaifu, N. *Astrophys. J.*, **1975**, *201*, L 149.
(56) Belsky, A. J.; Li, T. J.; Brill, T. B. *J. Supercrit. Fluids* **1997**, *10*, 201.
(57) Miller, S. L. *Biochim. Biophys. Acta* **1957**, *23*, 480.
(58) Miller, S. L.; Van Trump, J. E. In *Origins of Life*; Wolman, V., Ed.; D. Reidel Publ. Co.: Dorchecht, The Netherlands, 1981; p 135.
(59) Peltzer, E. T.; Bada, J. L.; Schlesinger, G.; Miller, S. L. *Adv. Space Res.* **1984**, *4*, 69.
(60) Cronin, J. R.; Chang, S. In *The Chemistry of Life's Origin*; Greenberg, J. M., Pirronella, V., Eds.; Kluver Academic: Dordrecht, The Netherlands, 1993; p 209.
(61) Kreible, V. K.; Noll, C. I. *J. Am. Chem. Soc.*, **1939**, *61*, 560.
(62) Lewan, M. D.; Fisher, J. B. In *Organic Acids in Geological Processes*; Pittman, E. D., Lewan, M. D., Eds.; Springer-Verlag: Berlin, 1994; Chapter 4.
(63) Shock, E. L. *Org. Life Evol. Biosphere* **1990**, *20*, 331.
(64) Bell, J. L. S.; Palmer, D. A. In *Organic Acids in Geological Processes*; Pittman, E. D., Lewan, M. D., Eds.; Springer-Verlag: Berlin, 1994; Chapter 9.
(65) Palmer, D. A.; Drummond, S. E. *Geochim. Cosmochim. Acta* **1986**, *50*, 813.
(66) Yu, J.; Savage, P. E. *Ind. Eng. Chem. Res.* **1998**, *37*, 2.
(67) Hirth, T.; Franck, E. U. *Ber. Bunsen-Ges. Phys. Chem.* **1993**, *97*, 1091.
(68) Falconer, J.; Madix, R. *Surf. Sci.* **1974**, *46*, 473.
(69) Maiella, P. G.; Brill, T. B. *Appl. Spectrosc.* **1996**, *50*, 829.